

# A simple empirical redshift indicator for gamma-ray bursts

J.-L. Atteia\*

Laboratoire d'Astrophysique, Observatoire Midi-Pyrénées, 31400 Toulouse, France

Received 3 April 2003 / Accepted 23 June 2003

**Abstract.** We propose a new empirical redshift indicator for gamma-ray bursts. This indicator is easily computed from the gamma-ray burst spectral parameters and its duration, and it provides “pseudo-redshifts” accurate to a factor two. Possible applications of this redshift indicator are briefly discussed.

**Key words.** gamma-rays: bursts

## 1. Introduction

Gamma-ray bursts (GRBs) are huge stellar explosions which have been observed at redshifts ranging from 0.0085 to 4.5. While GRBs are in principle detectable out to very large redshifts ( $z = 10\text{--}20$ , Lamb & Reichart 2000), redshifts measured to date do not exceed 4.5. The method most frequently used to measure GRB redshifts is to find a visible afterglow, and to identify absorption lines in its spectrum, caused by the gas in the GRB host galaxy. The redshift of the host can also be measured at late times from the host emission lines, when the afterglow has faded below detection. Another, less frequent, method uses X-ray lines detected in the X-ray afterglows of some GRBs. The absence of GRB detection beyond  $z = 5$  could be explained by the fact that the afterglows of such distant GRBs must be searched for in the infrared, due to the Lyman alpha cutoff. The difficulty to measure spectroscopic redshifts led various authors to propose alternate ways to determine GRB redshifts. Norris et al. (2000) and Reichart et al. (2001) have found empirical luminosity estimators based on GRB light curves. Such luminosity estimators can be used to infer the intrinsic luminosity of individual GRBs, and consequently their redshifts. While these estimators cannot be used to obtain precise redshifts for individual GRBs, they are useful to derive statistical properties of the GRB population.

Redshift estimators based on the gamma-ray data only present two distinctive advantages: they provide redshift estimates for most GRBs detected in gamma-rays, and they do not require extensive follow-up campaigns involving large telescopes on the ground or in space. Important issues can be addressed with moderately accurate redshifts, like the amount of energy released by GRBs in gamma-rays, the luminosity function of GRBs, or the history of stellar formation at high redshifts.

We propose here a new method to obtain redshift indicators for GRBs from gamma-ray observations. Our method is calibrated with 17 GRBs detected with BeppoSAX (Boella et al. 1997) and HETE (Ricker et al. 2001). In the following we call the redshifts inferred from our redshift indicator “pseudo-redshifts”. Pseudo-redshifts have the advantage of being very easily computed. In addition to the possible applications already mentioned, pseudo-redshifts may become a useful tool to quickly identify high-redshift GRBs.

## 2. An empirical redshift indicator

Finding redshift indicators for GRBs based on the gamma-ray data alone has always faced the problem of the large intrinsic dispersion of GRB properties. This intrinsic dispersion prevents the determination of the redshifts of individual GRBs. With the measure of an increasing number of GRB redshifts it appeared, however, that several properties of GRBs are correlated with the isotropic-equivalent energy radiated in gamma-rays (called  $E_{\text{rad}}$  in the following). For instance, the correlation of the spectral hardness with  $E_{\text{rad}}$  has been suspected for a long time (see e.g. Atteia 2000; Lloyd et al. 2000). It has only been demonstrated recently by Amati et al. (2002) for 12 GRBs with known redshifts. The correlation of the duration with  $E_{\text{rad}}$  is discussed in Lee et al. (2000). These correlations have led some authors to propose using the observed GRB properties to infer  $E_{\text{rad}}$ , and then to deduce the redshift from the comparison of the observed fluence with  $E_{\text{rad}}$ . Norris et al. (2000), for instance, estimate  $E_{\text{rad}}$  from the magnitude of the time lags between a high energy band and a low energy band. Reichart et al. (2001) estimate  $E_{\text{rad}}$  from the variability of the light curve. We propose and test here another approach: we search a quantity which depends little on  $E_{\text{rad}}$ , and which has a small intrinsic dispersion which does not blur the dependence on redshift. Starting from empirical considerations, We find such a quantity essentially based on the spectral characteristics of GRBs.

\* e-mail: [atteia@ast.obs-mip.fr](mailto:atteia@ast.obs-mip.fr)

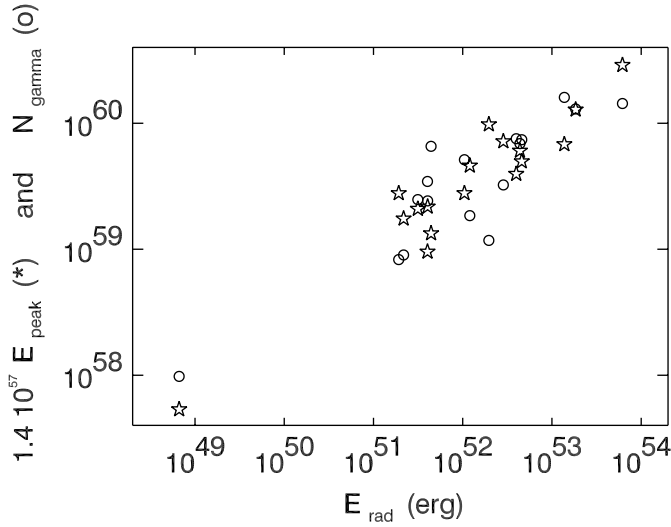


**Fig. 1.** Dependence of two characteristic GRB quantities on  $E_{\text{rad}}$ , the isotropic-equivalent energy radiated in gamma-rays. The stars show the dependence of the intrinsic peak energy (multiplied here by  $1.4 \times 10^{57}$ ). The circles show the dependence of the isotropic-equivalent number of photons emitted by the source.

GRB energy spectra are well fit with the so-called GRB model, consisting of two smoothly connected power laws (Band et al. 1993). In the following,  $\alpha$  is the index of the low-energy power law,  $\beta$  the index of the high-energy power law, and  $E_0$  is the break energy. With this parametrization, the peak energy of the  $\nu f_\nu$  spectrum is  $E_p = E_0 \times (2 + \alpha)$ .  $E_p$  is well defined for  $\alpha \geq -2$  and  $\beta < -2$ .

Our method is based on the recent finding by Amati et al. (2002) of a correlation between the intrinsic (redshift corrected)  $E_p$  of 12 GRBs with known redshifts, and  $E_{\text{rad}}$ , their isotropic-equivalent energy radiated in gamma-rays. According to Amati et al.,  $E_p$  is roughly proportional to the square-root of  $E_{\text{rad}}$ . Since  $\alpha$  and  $\beta$  do not vary too much from burst to burst, and since the energy radiated in gamma-rays is more or less the product of the number of photons by their typical energy, we make the assumption that the isotropic-equivalent number of photons in a GRB,  $N_\gamma$ , is also roughly proportional to the square-root of  $E_{\text{rad}}$ . For this study, we define  $N_\gamma$  as the number of photons below the break, integrated from  $E_p/100$  to  $E_p/2$ .

Figure 1 shows  $E_p$ , the intrinsic peak energy, and  $N_\gamma$ , the isotropic-equivalent number of photons as a function of  $E_{\text{rad}}$  for a sample of 17 GRBs detected by BeppoSAX, BATSE, and HETE. The main characteristics of these GRBs are given in Table 1, along with references for their spectral parameters. The redshifts have been taken from J. Greiner's GRB page at <http://www.mpe.mpg.de/~jcg/grbgen.html> (except for GRB 020124, which comes from Hjorth et al. 2003). Figure 1 shows that, as we suspected,  $E_p$  and  $N_\gamma$  have roughly the same dependence on  $E_{\text{rad}}$ . We can thus go one step further with our main conjecture: we suppose that the ratio  $N_\gamma/E_p$  is almost independent of  $E_{\text{rad}}$ , and can be used as a redshift indicator. Figure 2 shows that indeed the ratio  $N_\gamma/E_p$  shows very little dependence on  $E_{\text{rad}}$ , confirming our conjecture. This is not sufficient, however, to make it a correct redshift indicator. The critical issue is to find an indicator which has a small

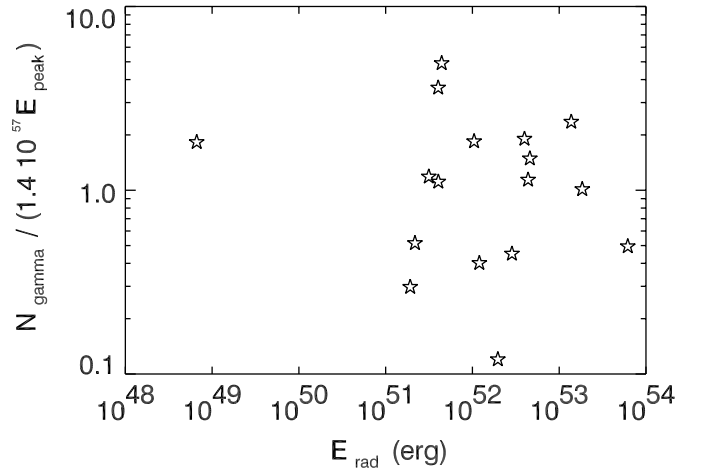


**Fig. 2.** The ratio  $N_\gamma/E_p$  (see text) as a function of  $E_{\text{rad}}$ . This figure illustrates the weak dependence of  $N_\gamma/E_p$  with  $E_{\text{rad}}$ .

**Table 1.** Observed properties of 17 GRBs with known redshift. The ten columns give the GRB name, the duration  $T_{90}$  in seconds, the three spectral parameters ( $\alpha$ ,  $\beta$ , and  $E_0$ ), the gamma-ray fluence  $S_\gamma$  in units of  $10^{-6}$  erg cm $^{-2}$ , the spectroscopic redshift  $z$ , the pseudo-redshift  $\hat{z}$ , the ratio  $\hat{z}/z$ , and a reference for the spectral parameters.

Name	$T_{90}$ s	$\alpha$	$\beta^a$	$E_0$ keV	$S_\gamma$	$z$	$\hat{z}$	$\hat{z}/z$	ref.
970228	80	-1.54	-2.5	250	11	0.695	0.94	1.36	1
970508	20	-1.71	-2.2	275	1.8	0.835	0.95	1.14	1
971214	35	-0.76	-2.7	125	8.8	3.42	2.87	0.84	1
980613	20	-1.43	-2.7	163	1.0	1.096	2.19	2.00	1
990123	100	-0.89	-2.45	703	300	1.60	2.20	1.38	1
990510	75	-1.23	-2.7	210	19	1.619	1.44	0.89	1
990705	42	-1.05	-2.2	199	75	0.843	0.85	1.01	1
990712	20	-1.88	-2.48	545	6.5	0.43	0.31	0.73	1
000131	96.3	-1.2	-2.4	163	26	4.5	1.35	0.30	2
010921	24.6	-1.49	-2.3	206	10.2	0.45	0.68	1.51	3
020124	78.6	-1.10	-2.3	133	6.8	3.2	2.17	0.68	3
020813	90	-1.05	-2.3	223	102	1.25	0.91	0.73	3
020903	9.8	-1.0	-2.3	3	0.09	0.25	0.26	1.03	4
021211	3.0	-0.896	-2.3	52	.96	1.01	0.76	0.75	5
030226	76.8	-0.95	-2.3	103	6.4	1.98	2.35	1.19	6
030328	140.	-1.0	-2.3	110	26.9	1.52	1.15	0.76	6
030329	22.8	-1.03	-2.26	59	118	0.168	0.17	0.99	7

<sup>a</sup>  $\beta$  has been frozen to  $-2.3$  for HETE GRBs 010921 to 030228.

- 1 Amati et al. (2002). Fluence measured in the range 40–700 keV.
- 2 Andersen et al. (2000). Fluence measured in the range 28–1800 keV.
- 3 Barraud et al. (2003). Fluence measured in the range 30–400 keV.
- 4 Sakamoto et al. (2003). Fluence measured in the range 7–30 keV.
- 5 Crew et al. (2003). Fluence measured in the range 7–30 keV.
- 6 Lamb et al. (2003). Fluence measured in the range 30–400 keV.
- 7 Vanderspek et al. (2003). Fluence measured in the range 7–30 keV.

dependence on  $E_{\text{rad}}$ , a strong dependence on the redshift, and a not too strong intrinsic dispersion. This issue is discussed in the next section.

### 2.1. Definition of the redshift indicator

The theoretical considerations in the previous section are based on the study of *intrinsic* GRB properties. Defining a redshift indicator implies that we do not know the redshifts of the GRBs which are being studied, but only their observed properties. To keep in mind this difference, in all the following we use capital letters for intrinsic quantities, and lower case for observed quantities.

As discussed earlier, the best redshift indicator is not necessarily the one with the smallest intrinsic dispersion, but rather the one which has the best combination of a small intrinsic dispersion and a large dependence on redshift. Relying on the analysis of the previous section, we propose to base our redshift indicator on  $n_\gamma/e_p$ , the ratio of the observed number of photons in the GRB on the observed peak energy. We tried various simple combinations of GRB parameters, all involving the ratio  $n_\gamma/e_p$ , and found that  $X = n_\gamma/e_p/\sqrt{t_{90}}$  has the right combination of properties for a redshift indicator. In this equation  $e_p$  is the observed peak energy,  $n_\gamma$  the observed number of photons between  $e_p/100$  and  $e_p/2$ , and  $t_{90}$  the observed duration. We do not claim here that  $X$  is definitely the best redshift indicator, we nevertheless believe that it is sufficiently good to deserve further discussion.

We derive pseudo-redshifts from the measure of  $X$  in the following way: in a first step we compute the theoretical evolution of  $X$  with redshift; then we invert this relation to derive a pseudo-redshift from the observed value of  $X$ . The evolution of  $X$  with redshift can be written as

$$X = A \times f(z)$$

$A$  is a constant of normalization, and  $f$  describes the evolution of  $X$  with redshift for a “standard” GRB ( $\alpha = -1.0$ ,  $\beta = -2.3$ , and  $E_0 = 250$  keV) in a “standard” universe ( $H_0 = 65$  km s<sup>-1</sup> Mpc<sup>-1</sup>,  $\Omega_0 = 0.3$ ,  $\Omega_\Lambda = 0.7$ ). GRB spectral parameters are not critical here, because we have shown in the previous section that the ratio  $N_\gamma/E_p$  does not vary much from burst to burst. The normalization constant  $A$  has been chosen to have about the same number of GRBs below and above the theoretical curve in Fig. 3 ( $A = 60$ ).

Pseudo-redshifts  $\hat{z}$  are then defined by

$$\hat{z} = \frac{1}{A} \times f^{-1}(X). \quad (1)$$

Their use as redshift indicators is discussed below.

### 2.2. Evaluation of pseudo-redshifts

Figure 3 shows the values of  $X$  as a function of  $z$ , for the 17 GRBs of Table 1. This figure displays a clear anticorrelation between the two quantities. The dotted line indicates the theoretical dependence  $X = A \times f(z)$ . The coefficient of correlation between  $z$  and  $X$  is  $-0.875$ , corresponding to a correlation significant at the level of 4.9 sigmas using Fisher’s  $Z$  transformation. We consider that this anticorrelation provides a good support to our intention of using  $X$  as a redshift indicator, and we use the Eq. (1) above to compute the pseudo-redshifts of GRBs in Table 1. Table 1 gives the values

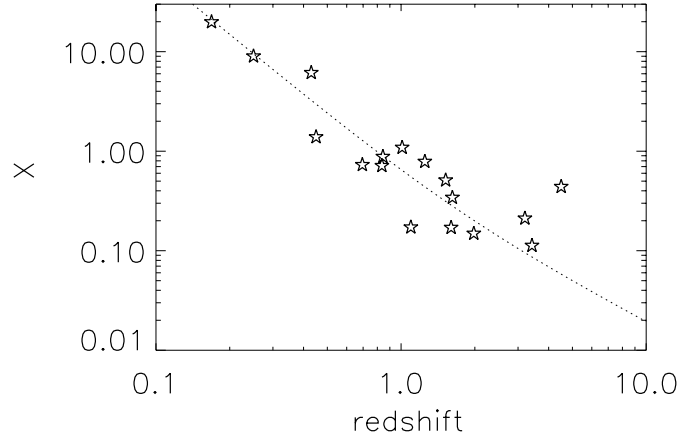


**Fig. 3.** Correlation of  $X = n_\gamma/e_p/\sqrt{t_{90}}$  (see text) with the measured redshifts of 17 GRBs. The isolated star at  $z = 4.5$  is GRB 000131. The dotted line shows the theoretical relation between  $\hat{z}$  and  $z$ .

of  $z$ ,  $\hat{z}$ , and their ratio, for the 17 GRBs with known redshift used in our analysis<sup>1</sup>. It shows that  $\hat{z}$  is usually within a factor of two of  $z$ , except for GRB 000131 (at  $z = 4.5$ ), for which  $z$  and  $\hat{z}$  differ by a factor 3.3. This discrepancy could be the consequence of the low quality of our redshift indicator for this burst (most probably) or of a problem with the measure of the spectral parameters of this GRB or of its redshift. It might also indicate that the relation between  $z$  and  $X$  is only working (or calibrated) to  $z = 3.5$ . Because this event is clearly an outlier, we recomputed the coefficient of correlation between  $z$  and  $X$  without it. We find a coefficient of correlation of  $-0.927$ , corresponding to a correlation significant at the level of 6.1 sigmas using Fisher’s  $Z$  transformation.

We conclude that the intrinsic dispersion of  $X$  is not such that it prevents its use as a redshift indicator. We prefer the term redshift indicator than redshift estimator, because the ratio of  $\hat{z}$  over  $z$  varies too much for a true redshift estimator. In the following we use the name pseudo-redshifts for  $\hat{z}$ . Because  $\hat{z}$  was derived from a purely empirical approach, we expect that an approach based on a physical treatment of GRB emission might provide a better redshift estimator. While pseudo-redshifts are a potentially useful tool, they deserve a word of caution here because we do not know how observational biases affect Fig. 3. We note for instance that GRBs with spectroscopic redshifts certainly represent a biased sample. In addition the relations linking the GRB properties (from which we compute  $X$ ) to those of their afterglows (from which we measure  $z$ ) are far from being understood. Anyone using this tool should thus keep in mind that Fig. 3 provides a biased view of the true distribution of GRBs in the  $(z, X)$  plane.

<sup>1</sup> Two GRBs in Amati et al. (2002) are not included in Table 1 because they do not have spectroscopic redshifts. The redshift of GRB 980326 was estimated to be 1 from the observation of a supernova bump in the late light curve of the afterglow (Bloom et al. 1999), and we find  $\hat{z} = 1.05$ . The redshift of GRB 000214 was estimated to be 0.42 from the observation of an iron line in its X-ray afterglow (Antonelli et al. 2000), and we find  $\hat{z} = 0.39$ .

**Table 2.** Observed properties of 18 GRBs with no measured redshift. The eight columns give the name of the GRB, the time of arrival, the duration  $T_{90}$  in seconds, the three spectral parameters ( $\alpha$ ,  $\beta$ , and  $E_0$ ), the gamma-ray fluence  $S_\gamma$  in units of  $10^{-6}$  erg cm $^{-2}$  in the range 30–400 keV, the pseudo-redshift  $\hat{z}$ , and a comment on the eventual detection of an afterglow (XRR stands for X-Ray Rich GRB, OA, XA, and RA, respectively for Optical Afterglow, X-ray Afterglow, and Radio Afterglow).

Name	Time SOD	$T_{90}$ s	$\alpha$	$E_0$ keV	$S_\gamma^e$	$\hat{z}$	Comment
001225	25 759	32.3	-1.17	283	114	0.64	
010126	33 162	7.7	-1.06	115	3.0	1.6	
010326A	11 701	23.0	-0.894	260	16	2.8	
010613	27 235	152.	-1.40	176	20.3	0.85	
010629	44 468	15.1	-1.17	59	2.6	0.76	XRR
010928	60 826	48.3	-0.623	260	21	4.9	
020113	7452	1.31	-0.46	239	1.3	2.3	Short/Hard
020127	75 444	9.3	-1.19	156	0.9	3.9	XA, RA, host
020214	67 778	27.4	-0.256	176	93	1.7	
020305	42 925	250.	-0.861	143	10.4	4.6	OA, host
020331	59 548	56.5	-0.922	120	4.5	3.4	OA
020418	63 789	7.54	-1.10	240	13.9	1.3	
020531	1578	1.15	-1.10	810	1.2	13.5	Short/Hard
020801	46 721	336.	-1.32	116	16.3	0.95	
020812	38 503	27.5	-1.03	125	2.3	3.4	
020819	53 855	33.6	-1.03	94	5.4	1.5	RA, host
021016	37 740	81.6	-0.98	132	11.3	2.1	
021104	25 262	19.7	-1.0	27	0.3	1.6	XRR

### 3. An example of using pseudo-redshifts

In this section we compute the pseudo-redshifts of 18 GRBs detected by HETE/FREGATE, whose spectral parameters are given in Barraud et al. (2003). We compare them with the pseudo-redshifts of 8 GRBs with known redshifts in Table 1 in order to assess the role of the redshift in the non-detection of the afterglows for these GRBs. The pseudo-redshifts of these 18 GRBs are given in Table 2.

The first remark is that short/hard GRBs should probably not be integrated in our framework. GRB 020531 for instance has a low  $X$  value, which results in an unrealistically high pseudo-redshift. Having no redshift for short/hard bursts we cannot evaluate, and eventually calibrate, our redshift indicator for these bursts. The two short/hard GRBs of our sample, GRB 020113 and GRB 020531, are thus excluded from the rest of our analysis.

The median pseudo-redshift of long GRBs in Table 2 is 1.65, while it is only 0.88 for the 8 FREGATE GRBs with a measured redshift in Table 1. If we believe the correlation between the pseudo-redshifts and the true redshifts, this indicates that the redshift certainly plays a role in the non-detection of the afterglows of FREGATE GRBs, even if this is not the only factor as emphasized by Crew et al. (2003).

While pseudo-redshifts can be useful for statistical analyses, the information they convey is probably not meaningful for individual GRBs. We believe however that pseudo-redshifts could become a useful tool to quickly identify high redshift

GRBs from the gamma-ray data alone. A first step in this direction is obviously to prove the validity of pseudo-redshifts for this task. GRB 020127 may appear as a good test case in this context because it has a high pseudo-redshift ( $\hat{z} = 3.9$  in Table 2), a possible X-ray afterglow, a possible radio afterglow, and a candidate host galaxy (Fox et al. 2002a, 2002b, 2002c). If the host candidate is at a redshift of about 3, this would strengthen the validity of pseudo-redshifts as a tool for the quick identification of high redshift GRBs.

### 4. Conclusion

We propose an empirical redshift indicator for GRBs, which is easily computed from the gamma-ray data alone and provides “pseudo-redshifts” accurate to a factor of two. Despite their moderate accuracy, we believe that their easy computation will make these pseudo-redshifts useful in future GRB studies. Their possible applications include a statistical comparison of the distance distribution of distinct GRB populations, constraints on the star formation rate at high redshifts, and the fast identification of remote GRBs, with redshifts beyond three.

The usefulness of these pseudo-redshifts will ultimately depend on the confirmation of their accuracy, which will be tested as a larger number of GRBs with known redshifts become available.

*Acknowledgements.* The author is grateful to R. Mochkovitch for insightful discussions on pseudo-redshifts and to C. Barraud for helpful suggestions. JLA acknowledges the use of J. Greiner GRB page at <http://www.mpe.mpg.de/~jcg/grbgen.html>, and useful comments from the referees.

### References

- Andersen, M. I., Hjorth, J., Pedersen, H., et al. 2000, A&A, 364, L54
- Amati, L., Frontera, F., Tavani, M., et al. 2002, A&A, 390, 81
- Antonelli, L. A., Piro, L., Vietri, M., et al. 2000, ApJ, 545, L39
- Atteia, J.-L. 2000, A&A, 353, L18
- Band, D., Matteson, J., Ford, L., et al. 1993, ApJ, 413, 281
- Barraud, C., Olive, J.-F., Lestrade, J. P., et al. 2003, A&A, 400, 1021
- Bloom, J., Kulkarni, S., Djorgovski, S., et al. 1999, Nature, 401, 453
- Boella, G., Butler, R., Perola, G., et al. 1997, A&AS, 122, 299
- Crew, G. B., Lamb, D. Q., Ricker, G. R., et al. 2003, ApJ, submitted
- Fox, D. W. 2002a, GCN 1249
- Fox, D. W., & Frail, D.A. 2002b, GCN 1250
- Fox, D. W., Djorgovski, S.G., & Kulkarni, S.R. 2002c, GCN 1306
- Hjorth, J., et al. 2003, Proc. of the 3rd workshop Gamma-Ray Bursts in the Afterglow Era, Roma 2002
- Lamb, D. Q., & Reichart, D. E. 2000, ApJ, 536, 1
- Lamb, D. Q., Sakamoto, T., Atteia, J.-L., et al. 2003, ApJ, submitted
- Lee, A., Bloom, E. D., & Petrosian, V. 2000, ApJS, 131, 21
- Lloyd, N. M., Petrosian, V., & Mallozzi, R. S. 2000, ApJ, 534, 227
- Norris, J., Marani, G., & Bonnell, J. 2000, ApJ, 534, 248
- Reichart, D., Lamb, D., Fenimore, E., et al. 2001, ApJ, 552, 57
- Ricker, G., Atteia, J.-L., Crew, G., et al. 2001, AIP Conf. Proc., 662, 3
- Sakamoto, T., Lamb, D. Q., Suzuki, M., et al. 2003, ApJ, submitted
- Vanderspek, R., Lamb, D., Sakamoto, T., et al. 2003, ApJ, submitted